Proceedings of the ASME 2010 3rd Joint US-European Fluids Engineering Summer Meeting and 8th International Conference on Nanochannels, Microchannels, and Minichannels
FEDSM-ICNMM2010
August 1-5, 2010, Montreal, Canada

FEDSM-ICNMM2010-30134

Creating Small Gas Bubbles in Flowing Mercury Using Turbulence at an Orifice

Mark Wendel[a] *Ashraf Abdou*[a] *Vincent Paquit*[a] *David Felde*[a] *Bernard Riemer*[a]

wendelmw@ornl.gov *ibrahimaa@ornl.gov* *paquitvc@ornl.gov* *feldedk@ornl.gov* *riemerbw@ornl.gov*

[a]*Oak Ridge National Laboratory*[1]*, Oak Ridge TN, USA*

ABSTRACT

Pressure waves created in liquid mercury pulsed spallation targets have been shown to create cavitation damage to the target container. One way to mitigate such damage would be to absorb the pressure pulse energy into a dispersed population of small bubbles, however, creating such a population in mercury is difficult due to the high surface tension and particularly the non-wetting behavior of mercury on gas-injection hardware. If the larger injected gas bubbles can be broken down into small bubbles after they are introduced to the flow, then the material interface problem is avoided.

Research at the Oak Ridge National Labarotory is underway to develop a technique that has shown potential to provide an adequate population of small-enough bubbles to a flowing spallation target. This technique involves gas injection at an orifice of a geometry that is optimized to the turbulence intensity and pressure distribution of the flow, while avoiding coalescence of gas at injection sites.

The most successful geometry thus far can be described as a square-toothed orifice having a 2.5 bar pressure drop in the mercury flow of 8 L/s for one of the target inlet legs. High-speed video and high-resolution photography have been used to quantify the bubble population on the surface of the mercury downstream of the gas injection site.

Also, computational fluid dynamics has been used to optimize the dimensions of the toothed orifice based on a RANS computed mean flow including turbulent energies such that the turbulent dissipation and pressure field are best suited for turbulent break-up of the gas bubbles.

1. INTRODUCTION

The Spallation Neutron Source (SNS) is an accelerator-based neutron source in Oak Ridge, Tennessee, USA. This one-of-a-kind facility (currently operating at 1 MW) provides the most intense pulsed neutron beams in the world for scientific research and industrial development [1]. Pulsed-proton-beam-induced heating of the SNS mercury target creates pressure waves that lead to the formation of cavitation bubbles in the mercury, which is flowing at 24 L/s through a stainless steel vessel as shown in Fig. 1. The inlet bulk flow (12 L/s in each leg) mercury Reynolds number is 2×10^5. The mercury makes a 180° turn against the front face of the target, called the window, where the inlet flows combine and return back through the larger center channel. Cavitation damage erosion (CDE) of the mercury container walls caused by violent collapse of these bubbles has been observed by post-irradiation examination of the first SNS target. This CDE potentially limits its power capacity and service lifetime [2].

Cavitation damage is reduced in the proximity of an extensive gas layer that overspreads the wall [5] using a gas retention strategy termed the gas-wall technique. This gas-wall

[1] Notice: This manuscript has been authored by UT-Batelle, LLC, under contract DE-AC05-00OR22725 with the U.S. Department of Energy. The United States Government retains, and the publisher, by accepting the article for publication, acknowledges that the United States Government retains a non-exclusive, paid-up, irrevocable, world-wide license to publish or reproduce the published form of this manuscript, or allow others to do so, for United States Government purposes.

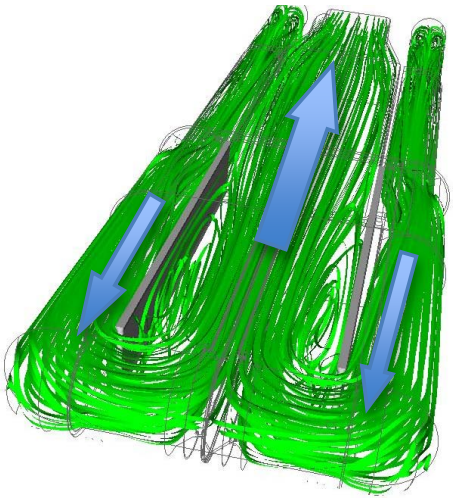

Figure 1. Bulk flow configuration for liquid mercury. Stream ribbons are shown as the two opposing inlet flows join into a common return channel.

technique has been demonstrated with enough success that an actual SNS target conceptual design effort is beginning to include it.

Another potential method to mitigate pitting damage on the target vessel is to inject small gas bubbles into the mercury at a sufficient void fraction to absorb the pressure wave resulting from the deposited beam energy [3, 4]. The desired bubble size for absorption of the proton beam energy is less than about 100μm [4]. However, there are other mechanisms [3] involving larger gas bubbles that could mitigate CDE as well. It is understood that to mitigate the damage by absorption, the gas must be located near the site at which a cavitation bubble forms and collapses. And, if the gas must be close to every cavitation site, then it stands to reason that the bubble size must be small in order to keep the total void fraction of the target small.

In creating small bubbles, complications arise due to the properties of mercury. First, injecting small bubbles is difficult since most injectors are made of materials that are not wetted by mercury, and those materials that are wetted are chemically consumed. With a non-wetted injector, such as stainless steel, the mercury/gas contact line expands along the surface of the solid (creating a greater retentive force) until fluid drag or buoyancy finally pulls the bubble away. During stagnant conditions this bubble size reaches a few millimeters even for injection through a thin needle. Other techniques to add forces or to induce wetting that would result in earlier bubble detachment have been attempted but are difficult to engineer and control, especially in situ at the SNS. It is therefore beneficial to use a simpler scheme that involves bulk fluid dynamic forces such as swirling [6], cavitation, or turbulence [7] to break the larger (millimeter scale) gas pockets into smaller bubbles that would be effective at mitigating the CDE.

Diagnostic development at ORNL is ongoing in parallel with the micro-bubbler development. Strategies include ultrasonic techniques and even proton radiography using a facility at Los Alamos National Laboratory (LANL), but direct observation of bubbles with high-speed cameras through a transparent window on the mercury surface has been the most reliable and convenient method of evaluating the performance of a given bubbler. For instance, the Target Test Facility (TTF) at ORNL (Fig. 2) has been fitted with a prototypical target that has 25-mm-thick acrylic windows on the top, through which the bubbles which make their way to the surface can be observed.

This paper discusses experiments with this TTF facility in developing a micro-bubble generator using a simple and convenient technique of helium gas injection through an inlet flow orifice that is designed to enhance turbulent break-up of the injected gas bubbles.

For turbulent break-up of the gas, the Martinez-Bazan correlation [7] has often been used to predict the equilibrium bubble size in a fully developed turbulent flow.

As applied to mercury, the Martinez-Bazan correlation is plotted in Fig. 3. This correlation is for fully developed and isotropic flow where all of the bubbles have enough time to reach their equilibrium size. In the present case, the region of turbulence is expected to be anisotropic and limited in extent near the orifice, so this correlation is expected to represent an

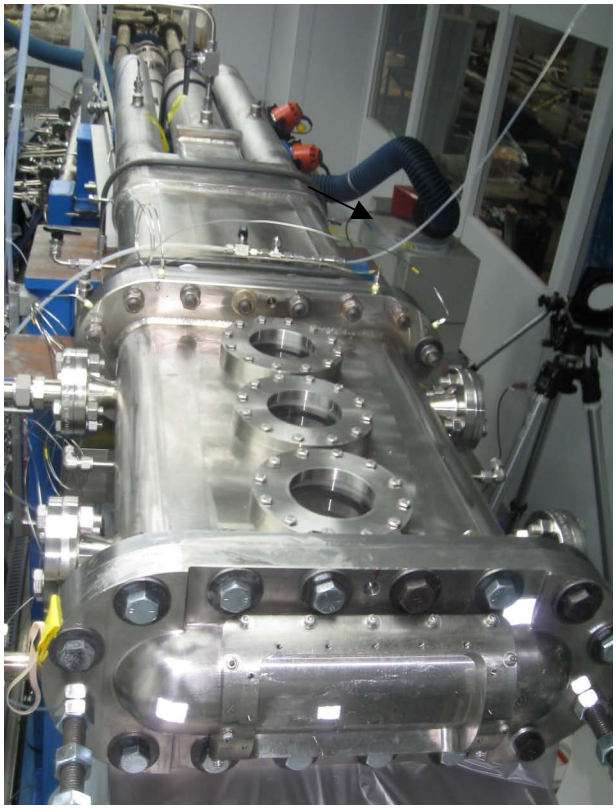

Figure 2. Target test facility with acrylic windows installed on top of the target. Gas feeds to eight orifice inlet bubblers are also visible. Only two were used here.

upper limit to the bubble sizes. Only the turbulent vortices that are of comparable span to the bubble size will be effective in breaking them up into smaller bubbles. As described by Anderssen et al [8], minimum activation energy is required in order to affect the break-up and then the energy level settles in to the new surface arrangement of the multiple bubble system. Turbulent velocity fluctuation covariance at an orifice is highly anisotropic just downstream of the edge [9], and this directional difference should distort the bubbles making them even more susceptible to break-up. So there are competing effects from conditions that should produce differences from Martinez-Bazan, and the results are obtained by physical experimentation.

This paper describes the experimental progress for one design of an inlet flow orifice gas injector. High-speed video was processed to quantify the downstream incident bubble flux as a function of bubble size on the acrylic windows. Also, CFD results are presented that show the optimization study for the bubbler design which helps to guide future experiments that are planned.

2. INLET ORIFICE GEOMETRY

The microbubble generator design investigated in this paper involves gas injection at two thick-walled orifices, located on each of the bulk flow inlets (Fig. 4). The orifices have rectangular teeth that provide small top areas (thickness × width) for gas injection that are subjected to high shear stress by the mercury flowing past, and induce intense (including cavitation) turbulent regions in the vicinity which should be effective to break down the bubble size.

The geometry of the inlet orifice is shown in Figs. 4, 5 and 6. The flange plate is 0.375-in. (9.53-mm) thick so that the gap cutouts between the teeth are cubic. The idea is to inject gas to the top of the tooth into the region of very high shear stress and low pressure. The size of the port through which the gas is fed is not very important, since the gas tends to spread along the non-wetted wall. The advantages of injecting the gas at the top surface are threefold:

(1) The sharp external corners of the tooth provide an edge that should stop the slide of the contact line and promote formation of small-scale turbulent structures.
(2) The tooth induces a local peak of wall shear stress and turbulent energy and dissipation just off of the wall that could serve in breaking down the bubble (will be discussed with CFD).
(3) The local static pressure is significantly reduced by 3 bar as the mercury speeds (near 7 m/s) past the edge of the tooth (mercury has S.G. = 13.6) so that the bubble size is initially inflated while it is broken down by the turbulence, only to shrink as the pressure recovers downstream. This lower pressure also pulls the gas away from the wall, promoting earlier bubble separation.

The inlet orifice Reynolds number is 2.4×10^6 where the average velocity in the cross-section is 4.7 m/s.

3. COMPUTATIONAL FLUID DYNAMICS

Computational fluid dynamics (CFD) has been used to simulate the single-phase behavior of the flowing mercury. These calculations have provided some guidance to the future research, and provide a diagnostic tool for probing inside the (opaque) mercury. The tooth dimensions have been optimized based on the CFD predictions, and a new orifice design will soon be tested.

The actual TTF flow (16 L/s divided into two inlet legs) was modeled with a Reynolds-averaged turbulence model in ANSYS-Fluent for single phase in order to predict the turbulent field. The goal of the analysis was to predict the tendency of the bubbles to break up due to local flow conditions. Cavitation was not modeled. Four grids (three hex grids and one with polyhedrals) were used to assure grid convergence. The resulting extrema just off the surface of the tooth (Fig. 7 shows the peaks in eddy dissipation) are shown in Table 1.

The computed profiles appear qualitatively similar to turbulent mixing results published by Mi et al [9, 10] for experiments in air with notched orifices. As explained by Mi et al, the notched jet enhances mixing through greater entrainment and the corners lead to more production of fine-scale turbulence.

Table 1. Local extrema for dependent variables in the CFD for the prototypical target with inlet orifice bubblers.

Velocity maximum	6.9 m/s
Pressure minimum (with respect to target outlet)	-1.2 bar
Turbulence intensity maximum	64%
Turbulent kinetic energy maximum	0.6 m^2/s^2
Turbulence dissipation maximum	1140 m^2/s^3

These peaks are much more intense near the square teeth than similar peaks for a simple circular orifice without teeth. As shown in Fig. 3, using Martinez-Bazan at this value for eddy dissipation, large, millimeter-sized bubbles should be expected.

An optimization study was performed at 1/3 scale with future experimental apparatus in mind. For the optimized case, the local peaks just off the surface of the tooth are shown in Table 2. This increased energy in the smaller length scales is expected to lead to smaller bubble sizes, and Fig. 3 would indicate 100 micron scale bubbles should be produced. Designs that utilize a different shape for the tooth are also being considered. As previously stated, the Martinez-Bazan

correlation is based on fully developed isotropic flow without cavitation, and with no direct way to quantify the efficiency of the bubble break-up using the simple single-phase RANS CFD, an experiment was performed and the bubbles were photographed and analyzed using image processing.

Table 2. Local extrema for dependent variables in CFD for the 1/3 scale circular orifice optimized.

Velocity maximum	7 m/s
Pressure minimum (with respect to the target outlet)	-1.6 bar
Turbulence intensity maximum	125%
Turbulent kinetic energy maximum	2.4 m^2/s^2
Turbulence dissipation maximum	13,000 m^2/s^3

4. EXPERIMENTAL RESULTS

Using the TTF facility of Fig. 2, high speed video images were obtained at 1000 frames per second through the acrylic windows (Fig. 8 shows bubbles on window) during operation of the bubblers at nominal flow conditions. The window is located 75 cm downstream of the bubbler, past a U-turn in the target. A helium gas flow rate of 20 sccm was used on only two of the eight injection locations. This injection rate produces 3×10^{-5} void fraction of helium. Although observations of the surface flux for the bubble population will be different from the bulk population, a strong correlation between the two must exist, and work is underway to correlate the two more precisely by using other diagnostics, CFD and analogies with water where bubbles can be seen inside. The surface technique used here should be helpful in comparing the performance of different micro-bubblers.

The video was analyzed using MATLAB® Image Processing capabilities. Here, the height of the field of view is only 1.7 cm (Fig. 9), making a pixel size about 40 microns. In order to track and to perform quantitative measurements of the bubbles arriving on the surface of the window, a four-phase image processing method was used: (1) registration, (2) segmentation, (3) tracking, and (4) quantification.

The high-speed camera is positioned above the acrylic window embedded in the target casing, which vibrates due to the turbulence of the mercury flow. This vibration creates sideways translations of the images in the video sequence, a phenomenon that is amplified with increased magnification required for identifying very small bubbles. The first phase of the method consists of image registration across the video sequence in order to compensate for vibrations. Figure 9 is the first image of the 1000 fps video sequence where one can see a high density of scratches (white stripes) on the surface of the window. Across the video sequence, the total surface covered by scratches is significantly higher than the surface covered by bubbles. Therefore, bubbles can be considered as noise on the top of the scratched window images. The images are registered by considering the defects as a support for a matching algorithm. Using the cross-correlation between a reference image, i.e. the first image of the sequence, and all the remaining, a transformation function is calculated. Based on the maximum deviation in the sequence, the video is then cropped accordingly in order to remove the missing pixel effect at the border. A video is then produced where all the scratches are static across the sequence and in which the bubbles are the only entities moving. Bubbles that remain affixed to the window throughout the video sequence are not counted, and are considered as part of the background. The background image is then computed as the average image across the video sequence.

The segmenting step is next: the background image is subtracted from each frame and the bubbles are identified as the regions where the pixel intensity crosses a defined threshold. Bubble tracking and quantitative measurement is then performed. At the 1000 fps frame rate, the maximal average bubble-centroid displacement is 2-3 pixels from one frame to the next. By assigning a label to each newly detected bubble, assigning the same label to bubbles present in consecutive frames whose centroid lies close-by, and by following them over time, the bubble trajectories are computed.

Finally, each bubble is analyzed independently. The end goal is to isolate the bubbles coming from the mercury flow and appearing directly on the window surface. After categorizing the bubble trajectory, the size and shape and morphology are computed. In the end, a full characterization of the bubbler performance is available that can be used to rank the micro-bubblers from best to worst in terms of their ability to create large populations of small bubbles.

For the inlet orifice bubbler that is the topic of this paper, the results are shown in Fig. 10 with only two of the bubblers active. The symbols in Fig. 10 show the center range of the bins into which the bubbles were placed based on their sizes. The sampling time is 2 s at 1000 fps and 267 bubbles are observed to enter the viewing window. The figure strongly implies that even smaller bubbles probably exist that are below the pixilation limit. With such a stark difference between what would be predicted by turbulent stresses, it is possible that dynamic two-phase effects may play a big role in reducing the bubble sizes. It may be the case that cavitation is actually responsible for the creation of the smallest micro-bubbles.

5. CONCLUSION

Experiments performed at the ORNL have demonstrated that micro-bubbles as small as 40 microns are created in flowing mercury with a square-toothed inlet orifice, well below the bubble size predicted by turbulent-breakup models for isotropic fully developed turbulent flow. CFD results have helped explain the success and allowed for optimization of

future experiments. Also, an image-processing algorithm has been created that will be useful in quantifying micro-bubble generator performance in upcoming development. Although the processed population, which is based on observations on the surface, may not be exactly that of the bulk, there should be a strong correlation. This particular micro-bubbler design is a reasonable option for gas injection to mitigate cavitation damage on the SNS target and has the advantage that it can easily be integrated into the SNS flow loop design inside of the replaceable target module. It remains to be shown whether this small gas bubble population will actually mitigate cavitation damage. In-beam testing of the concept will occur in the near future.

REFERENCES

1. neutrons.ornl.gov
2. Haines, J.R., Riemer, B.W., Felde, D.K., Hunn, J.D., Pawel, S.J. and Tsai, C.C., "Summary of Cavitation Erosion Investigations for the SNS Mercury Target", Journal of Nuclear Materials, vol. 343, pp. 58–69, 2005.
3. Ishikura, S. et al, Bubble dynamics in the thermal shock problem of the liquid metal target , Journal of Nuclear Materials, vol. 318, 15, pp. 113-121, 2003.
4. Futakawa, M. et al, R&D on pressure wave mitigation techniques in mercury targets, ICANS-XVIII, 18th Meeting of the International Collaboration on Advanced Neutron Sources, Dongguan , Guangdong Province, P.R. China, April 26-29, 2007.
5. Wendel, M. W. et al, Progress in Establishing Gas Layer in a Flowing Mercury Target, ASME 2008 Fluids Engineering Division Summer Meeting, Jacksonville, FL.
6. Tabei, K. et al, Study of microbubble generation by a swirl jet, Journal of Environment and Engineering, vol.1, 1, pp. 172-182, 2007.
7. Martinez-Bazán, C. et al, On the break-up of an air bubble injected into a fully developed turbulent flow Part I: Break-up frequency, Journal of Fluid Mechanics, 401, pp. 157-182.
8. Andersson, R. and B. Andersson, On the breakup of fluid particles in turbulent flows, AIChE Journal, vol. 52, 6, pp. 2020-2030, June, 2006.
9. Morrison, G. et al, Mean velocity and turbulence fields inside a β=0.5 orifice flowmeter, AIChE Journal, vol. 39, 5, pp. 745-756, May 1993.
10. Mi, J., Kalt, J. and Nathan, G., On Turbulent Jets Issuing from Notched-Rectangular and Circular Orifice Plates, J Flow Turb and Comb, Published Online, 27 October 2009.
11. Mi, J., Kalt, J. and Nathan, G., Near-Field Mixing Characteristics of Turbulent Jet Issuing from a Notched-Rectangular Orifice Plates, Proceedings of the Fifth International Conference on Fluid Mechanics, Shanghai, China, Aug. 15-19, 2007.

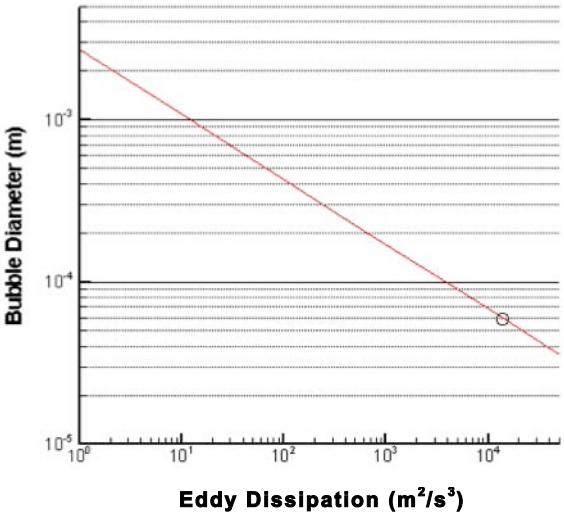

Figure 3. Martinez-Bazan correlation for applied to mercury at room temperature.

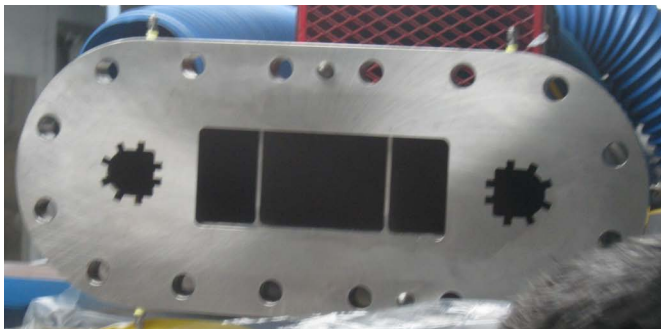

Figure 4. Flange containing square-toothed orifice inlet bubblers.

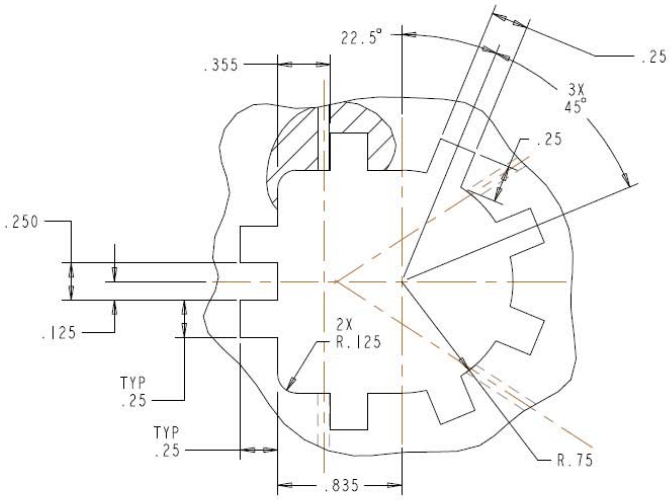

Figure 5. Dimensions (inches) on the square-toothed D-shaped orifice that was operated in TTF. Gas injection holes are also indicated.

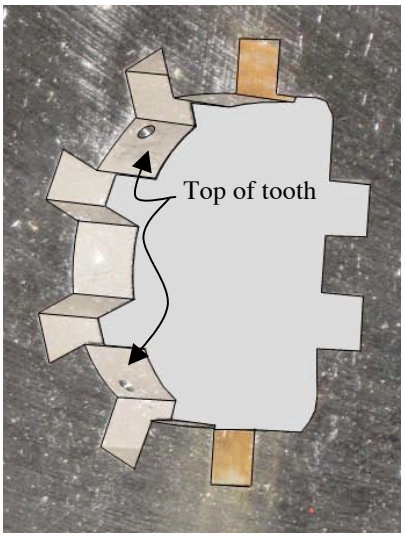

Figure 6. Square-toothed orifice with two of the four gas-injection holes visible.

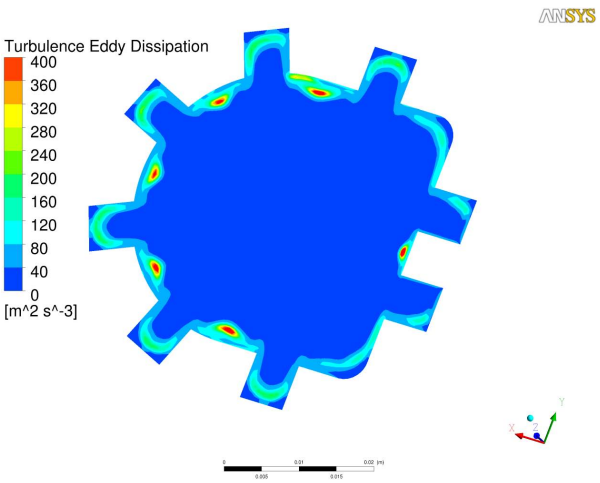

Figure 7. CFD results showing turbulent eddy dissipation rate for target inlet orifice with local maximum off of the surface of the teeth.

Figure 8. Single frame of high-speed video through acrylic window (diameter of 83 mm) with a view to bubbles in mercury on top side of target.

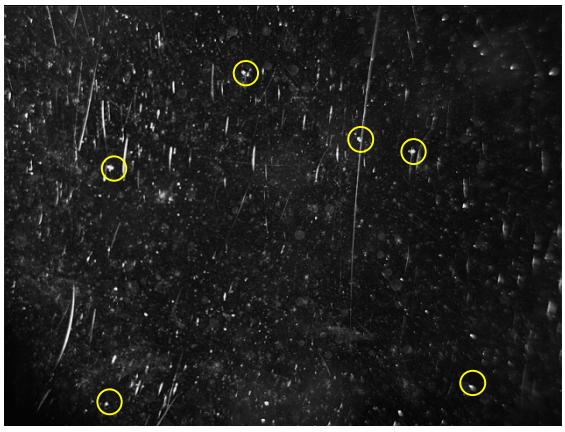

Figure 9. Single frame of high-speed video through acrylic window at higher magnification (frame height is 1.7 cm). Bubbles are circled.

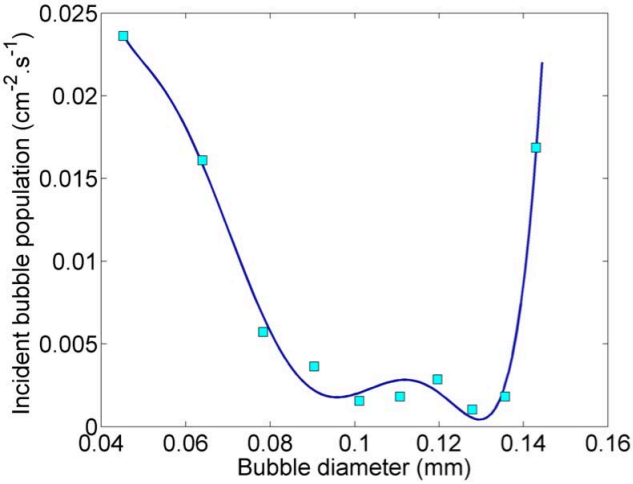

Figure 10. Bubble population incident on the observation port for 2 nozzles at 20 sccm each in the square-toothed inlet orifice bubbler.